Aalborg Universitet

AALBORG UNIVERSITY
DENMARK

Experimental Study of Wind-Opposed Buoyancy-Driven Natural Ventilation

Andersen, A.; Bjerre, M.; Chen, Z. D.; Heiselberg, Per; Li, Y.

[Link to publication from Aalborg University](#)

Experime

Experimental Study of Wind-Opposed Buoyancy-Driven Natural Ventilation

A. Andersen, M. Bjerre, Z.D. Chen,

P. Heiselberg, Y. Li

Experimental Study of Wind-Opposed Buoyancy-Driven Natural Ventilation

A. Andersen, M. Bjerre, Z.D. Chen,

P. Heiselberg, Y. Li

INNOVATIONS IN VENTILATION TECHNOLOGY

21st ANNUAL AIVC CONFERENCE
THE HAGUE, NETHERLANDS, 26–29 SEPTEMBER 2000

Experimental Study of
Wind-Opposed Buoyancy-Driven Natural Ventilation

A. Andersen[1], M. Bjerre[2], Z. D. Chen[3], P. Heiselberg[4], Y. Li[5]

[1] WindowMaster A/S
Skelstedet 13, 2950 Vedbæk, Denmark

[2] Brix & Kamp A/S
Nørregade 27, 9800 Hjørring, Denmark

[3] Thermal and Fluids Engineering
CSIRO Building, Construction and Engineering
PO Box 56, Highett, Victoria 3190, Australia

[4] Indoor Environmental Engineering
Department of Building Technology and Structural Engineering
Aalborg University, Sohngaardsholmsvej 57, DK-9000 Aalborg, Denmark

[5] Department of Mechanical Engineering
The University of Hong Kong
Pokfulam Road, Hong Kong

1. INTRODUCTION

Natural ventilation driven by natural forces, i.e. wind and thermal buoyancy, is an environmentally friendly system for buildings and has been increasingly used around the world in recent years to mitigate the impact on the global environment due to the significant energy consumption by heating, ventilation and air-conditioning (HVAC). There is a need for the understanding and development of theories and tools related to the design, operation and control of natural ventilation systems.

Considering the combined effect of natural forces, wind can either assist or oppose thermal buoyancy, and thus result in three different modes of ventilation flow, as shown in Figure 1. In the case of assisting winds, there is only one possible ventilation flow direction, i.e. upward flow (refer to Figure 1A). For opposing winds there are two possible flow directions, depending on the dominating force: downward flow for wind-dominated ventilation (Figure 1B) and upward flow for buoyancy-dominated ventilation (Figure 1C).
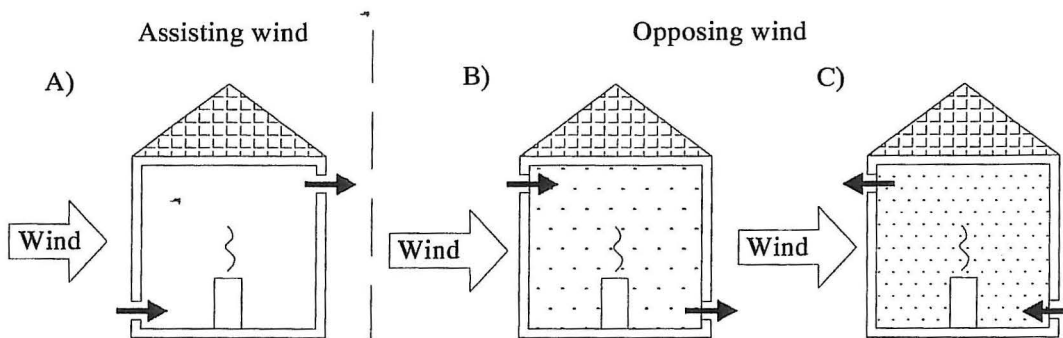

Figure 1. Directions of natural ventilation flow with assisting and opposing winds. The intensity of the dots in the rooms with opposing wind illustrates the inside temperature – the higher the intensity, the higher the temperature.

Hunt and Linden (1997) and Linden (1999) investigated wind-assisted buoyancy-driven natural ventilation in a single-zone building and good agreement was obtained between their theoretical predictions and experimental results from a salt-bath modelling system.

Li and Delsante (1998) presented a theoretical analysis of wind-opposed buoyancy-driven natural ventilation and found that multiple solutions exist for a single-zone building with two vertically displaced openings. It was also shown that for a given ventilation mode, the ventilation flow rate is determined by three characteristic parameters, i.e. the buoyancy air change parameter (α), the wind air change parameter (γ) and the envelope heat loss parameter (β). The definitions of the three parameters are shown in Table 1 together with their practical ranges.

Figure 2 shows the analytical solutions for $\beta = 0$, i.e. without heat loss through the building envelope. It is seen that there are multiple solutions for a range of α/γ from 0 to 1. α/γ represents the relative strength between the buoyancy and the wind. The curve between B and E in Figure 2 was proved to be unstable (Li and Delsante 1998).

Table 1. Parameters determining ventilation flow rate.

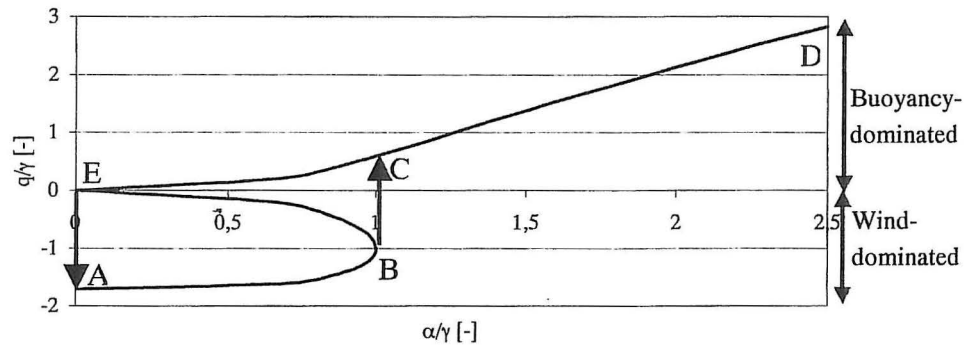| Name	Dimension	Symbol	Equation	Range
Buoyancy air change parameter	m^3/s	α	$\alpha = \left(C_d \cdot A^*\right)^{2/3} \cdot \left(\dfrac{\Phi_{total} \cdot g \cdot H}{\rho \cdot c_p \cdot T_o}\right)^{1/3}$	0–4.5
Envelope heat loss parameter	m^3/s	β	$\beta = \sum\limits_{j=1}^{j=n} U_j \cdot A_j \cdot \left(3 \cdot \rho \cdot c_p\right)^{-1}$	0–0.1
Wind air change parameter	m^3/s	γ	$\gamma = 3^{-0,5} \cdot \left(C_d \cdot A^*\right) \cdot \sqrt{2 \cdot \Delta P_w}$	0–16

Figure 2. Non-dimensional ventilation flow rate q/γ as a function of the non-dimensional buoyancy air change parameter α/γ.

Referring to Figure 2, let's start from wind-dominated flow and zero buoyancy force, i.e. point A, the non-dimensional ventilation flow rate q/γ starts from point A towards points B, C and D as the buoyancy flux increases. Between points B and C the flow changes direction from a wind-dominated to a buoyancy-dominated flow. This point is referred to as the turning point. For $\beta = 0$, i.e. without heat loss through the building envelope, the turning point is predicted to occur at $\alpha/\gamma = 1.0$. As the buoyancy flux decreases from point D, the flow remains buoyancy-dominated until the buoyancy flux approach zero (point E), where it may change to wind-dominated again (point A) with any small flow disturbances.

In Li and Delsante's analytical solution the indoor air was assumed to be fully mixed, i.e. with a uniform air temperature. For wind-dominated flow, a fully mixed flow pattern is a reasonable assumption. However, in the case of buoyancy-dominated flow, the air can be characterised as stratified, with a horizontal stratification interface at a certain level of the building, depending on the buoyancy strength and the building geometry. Improved analysis which takes temperature stratification into account has recently been carried out (Li and Delsante 1999; Andersen and Bjerre 2000). Figure 3 shows a comparison of the solutions obtained by the two analyses. As discussed above, there is no difference between the two analyses for wind-dominated ventilation flow. It was found that while a lower ventilation flow rate is obtained for the buoyancy-dominated ventilation mode with the consideration of temperature stratification, the occurrence of multiple solutions still exists.

Consequently, from both analyses, it was predicted that different ventilation history and operation will result in two totally different stable ventilation pattern and thus ventilation

flow rate at otherwise exactly the same building geometry, wind and thermal conditions. The findings of Li and Delsante are perhaps significant considering the design and especially the operation and control of natural ventilation systems. The conventional design methods do not show the existence of multiple solutions. In this paper, an experimental study was carried out to investigate whether multiple solutions occur in a scaled building model with wind-opposed buoyancy-driven natural ventilation.
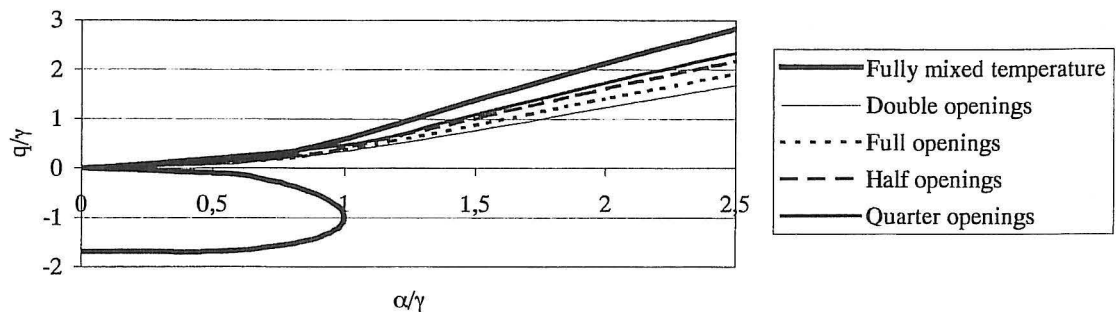
Figure 3. A comparison of the non-dimensional ventilation flow rate predicted by analyses with fully mixed and stratified flow assumption for buoyancy-dominated flow. Here full opening refers to $C_d A^*/H^2 = 0.003$.

2. EXPERIMENTAL

Experimental modelling was performed in the CSIRO Thermal and Fluids Laboratory using a single-zone building model with two vertically displaced openings and a point buoyancy source in the middle of the floor, as illustrated in Figure 4. The model was made of perspex to allow particle image velocimetry (PIV) measurements and visualisations of the flow field, and it is scaled at 1:50 compared to a typical atrium ($h \times w \times l = 10$ m $\times$ 10 m $\times$ 5 m).

Figure 4. Illustration of the small-scale model.

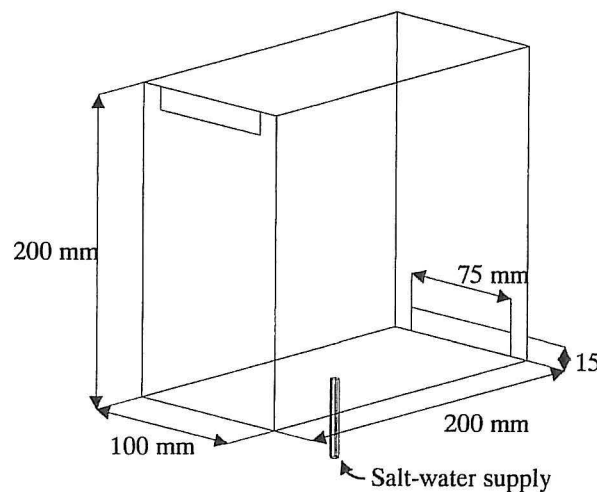The salt-bath technique is used to simulate the heat source in the model. Since salt water is denser than fresh water and hot air is lighter than cold air, the model is immersed upside down in the water. By injecting salt water into the model through a small opening at the floor, a turbulent plume is generated which simulates a thermal plume rising from a heat source.

The model was arranged in the test section of a water tunnel in order to simulate the wind affect around the building. A schematic view of the experimental arrangement is illustrated in Figure 5. The water tunnel contains 3 m^3 of water, which is necessary in order to remain a relatively constant density of the ambient fluid during the experiment.
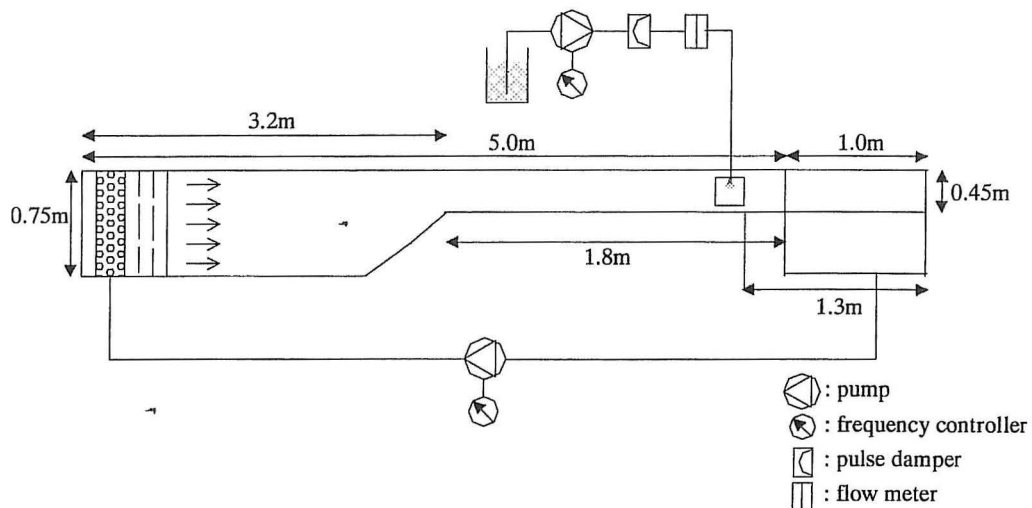

Figure 5. Schematic view of the experimental set-up.

Flow visualisation is achieved by adding dye into the building as well as using a shadow-graph technique. With this shadow-graph technique the flow patterns are illustrated as shadows on a white paper by casting light on the paper through the salt water in the model.

Before the experiments, calibrations were carried out for the water tunnel velocity, the salt-water density and the volumetric meter of the salt-water injection system. The natural ventilation flow rate through the building openings was measured by PIV.

3. RESULTS AND DISCUSSION

3.1 Visual Observations

The tests are performed with a variable internal heat source at a fixed wind speed around the building. This is chosen since the time for achieving a steady state in the system is shorter with changes in the buoyancy source (15 minutes) than changes in the wind speed (30 minutes).

A typical experiment begins with a wind-dominated ventilation mode without any heat source, i.e. stage *O* in Figure 6. Then the 'heat' source is gradually increased by supplying salt water into the model building, i.e. stages *A*, *B* and *C* in Figure 6, until the flow reaches

the turning point and becomes buoyancy-dominated, i.e. stage D. Then the supply of salt water is decreased, but the ventilation remains buoyancy-dominated until the stratification layer reaches the inlet opening even though the supply of salt water is very small, i.e. stage E in Figure 6.

Observations of the flow patterns at different stages as shown in Figure 6 clearly indicate the existence of multiple solutions. This was further confirmed with different combinations of the internal buoyancy source strength at three different wind speeds. As shown in Figure 6, stages $A–C$ are wind-dominated flow and the fluid in the building is well mixed. Stages $D–E$ are buoyancy-dominated ventilation and the fluid in the building is stratified. From Figure 6, it is also seen that when the buoyancy flux is relatively small, the jet caused by the surrounding wind from the inlet has a long penetration length before it declines in the room. As the buoyancy flux increases, the penetration length decreases due to the increasing density difference between the fluids inside and outside the room, as well as the higher momentum flow induced by the buoyancy source.
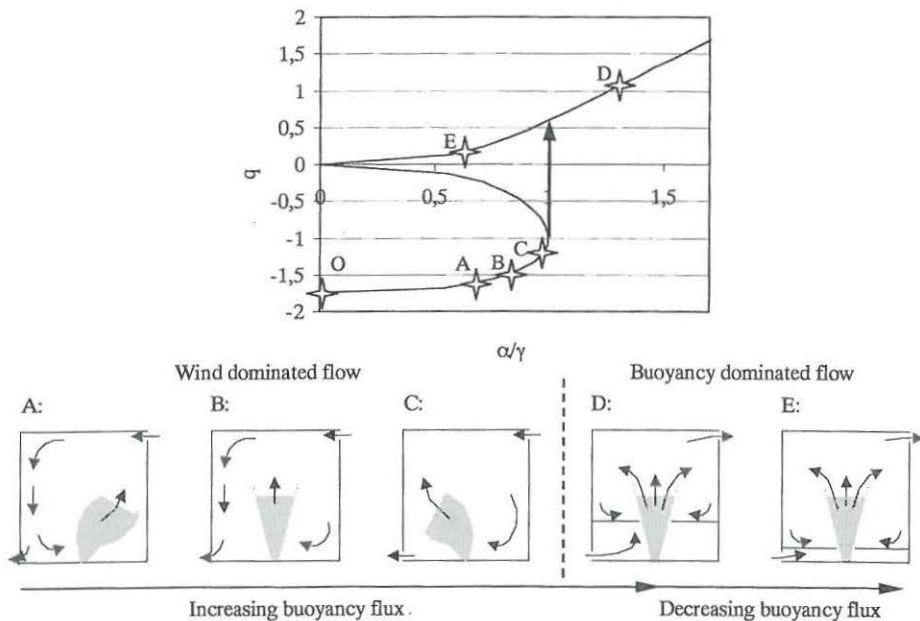
Figure 6. Flow patterns in the model at different stages.

3.2 Turning Points

The turning point from wind- to buoyancy-dominated flow is obtained for different combinations of wind, internal heat source and opening height. As shown in Table 2, the non-dimensional parameter α/γ at the turning point is independent of wind speed, internal heat source and opening height, as expected from the analyses as shown in Figures 2 and 3. The mean value of α/γ for eight different tests is 1.06, which is 6% higher than the theoretical

prediction of 1.0 as shown in Figures 2 and 3. This difference may be caused by at least two factors: (1) the perfect mixing assumption in the analysis for wind-dominated ventilation is not likely to be achieved in reality; and (2) experimental uncertainty, which is around 10% depending on the measurement accuracy of the buoyancy flux and the pressure difference over the two openings.

Table 2. The non-dimensional parameter α/γ at the turning point for different buoyancy, wind and opening sizes.

Test no.	Mean velocity in the water tunnel [m/s]	Salt solution		Turning point α/γ [–]
		Density [kg/m^3]	Volume flow rate [l/h]	
1	0.06	1016	9.0	1.056
2	0.07	1016	14.3	1.051
3	0.08	1032	11.0	1.057
4	0.09	1032	16.2	1.066
5	0.09	1064	8.2	1.070
6	0.10	1064	10.6	1.033
7*	0.08	1016	9.8	1.049
8*	0.10	1032	10.2	1.029

* Half opening height (7.5 mm).

3.3 Ventilation Flow Rate

PIV measurements of the ventilation flow rate were performed for two opening heights, i.e. 15 mm and 7.5 mm respectively. In Figure 7, the experimental results are shown together with the predictions from both analyses. It is seen that the experimental results are in reasonable agreement with both analyses, and as expected a better agreement was found between the experiments and the analysis considering temperature stratification.
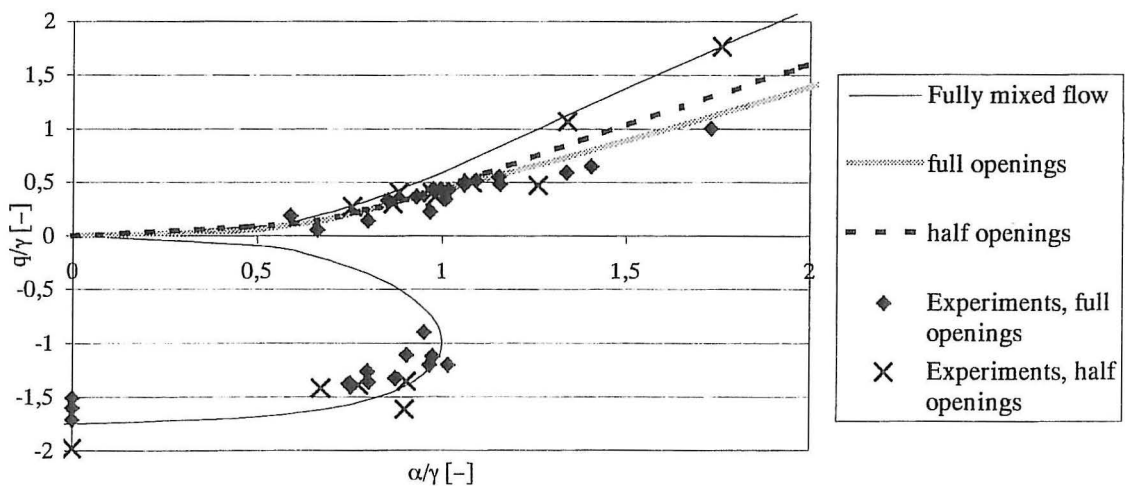

Figure 7. Comparison between the experimental ventilation flow rate and the analytical predictions.

From Figure 7, it can also be seen that experimental results for the half-opening size approach the predictions by the analysis with the fully mixed assumption. The reason for this is that when the opening size becomes smaller, the stratification interface height for buoyancy-dominated ventilation (refer to Figure 6D) is lower. Consequently, the bulk of the fluid in the building can be essentially approximated by the fully mixed assumption.

4. CONCLUSION

Experimental modelling of wind-opposed buoyancy-driven natural ventilation in a single-zone building confirmed the existence of two possible flow modes and thus two different flow rates in a certain range of thermal buoyancy and wind conditions. The experimental results obtained for both the turning point value and the ventilation flow rate are in good agreement with the theoretical predictions of Li and Delsante (1998; 1999) and Andersen and Bjerre (2000).

It was also demonstrated that when multiple ventilation modes exist, the final steady state ventilation mode and thus the ventilation flow rate are dependent on the ventilation history of the building. The existence of multiple solutions, as demonstrated in the analysis of Li and Delsante (1998; 1999) and the experimental results in this work, suggests that care should be taken in the design of natural ventilation systems – especially the design of the operation and control systems.

5. REFERENSES

Andersen, A. and Bjerre, M.: Natural Ventilation Induced by Combined Wind and Thermal Forces, Internal Report 00/50, CSIRO Building, Construction and Engineering, Australia, 2000.

Li, Y. and Delsante, A.: On Natural Ventilation of a Building with Two Openings. Proceedings 19th AIVC Conference, 'Ventilation Technologies in Urban Areas', Oslo, Norway, 28–30 Sep. 1998, pp. 189–196.

Li, Y. and Delsante, A.: Natural Ventilation Induced by Combined Wind and Thermal Forces in Buildings with Thermal Stratification. Unpublished paper draft, CSIRO, Division of Building, Construction and Engineering, Australia, 1999.

Hunt, G.R. and Linden, P. F.: Passive Cooling by Natural Ventilation: Salt Bath Modelling of Combined Wind and Buoyancy Forces. Proceedings of the 18th Annual AIVC Conference, Athens, Greece, 23-26, September, 1997.

Linden, P. F.: The Fluid Mechanics of Natural Ventilation, Annual Rev. Fluid Mech., vol. 31, pp. 201–238, 1999.

RECENT PAPERS ON INDOOR ENVIRONMENTAL ENGINEERING

PAPER NO. 109: E. Bjørn: *Simulation of Human Respiration with Breathing Thermal Manikin*. ISSN 1395-7953 R9944.

PAPER NO. 110: P. Heiselberg: *Hybrid Ventilation and the Consequences on the Development of the Facade*. ISSN 1395-7953 R0033.

PAPER NO. 111: P. Heiselberg, M. Pedersen, T. Plath: *Local Exhaust Optimization and Worker Exposure*. ISSN 1395-7953 R0034.

PAPER NO. 112: K. Svidt, P. Heiselberg: *Push-Pull Ventilation in a Painting Shop for Large Steel Constructions*. ISSN 1395-7953 R0035.

PAPER NO. 113: P. Heiselberg: *Design Principles for Natural and Hybrid Ventilation*. ISSN 1395-7953 R0036

PAPER NO. 114: A. Andersen, M. Bjerre, Z.D. Chen, P. Heiselberg, Y. Li: *Experimental Study of Wind-Opposed Buoyancy-Driven Natural Ventilation*. ISSN 1395-7953 R0037

PAPER NO. 115: P. Heiselberg, K. Svidt, P.V. Nielsen: *Windows - Measurements of Air Flow Capacity*. ISSN 1395-7953 R0040

PAPER NO. 116: K. Svidt. P. Heiselberg, P.V. Nielsen: *Characterization of the Airflow from a Bottom Hung Window under Natural Ventilation*. ISSN 1395-7953 R0041

PAPER NO. 117: Z. Yue, P.V. Nielsen: *Flow Pattern in Ventilated Rooms with Large Depth and Width*. ISSN 1395-7953 R0042.

PAPER NO. 118: P.V. Nielsen, H. Dam, L.C. Sørensen, K. Svidt, P. Heiselberg: *Characteristics of Buoyant Flow from Open windows in Naturally Ventilated Rooms*. ISSN 1395-7953 R0043.

PAPER NO. 119: P.V. Nielsen, C. Filholm, C. Topp, L. Davidson: *Model Experiments with Low Reynolds Number Effects in a Ventilated Room*. ISSN 1395-7953 R0044.

PAPER NO. 120: P. Lengweiler, P.V. Nielsen, A. Moser, P. Heiselberg, H. Takai: *Experimental Method for Measuring Dust Load on Surfaces in Rooms*. ISSN 1395-7953 R0045.

PAPER NO. 121: L. Davidson, P.V. Nielsen, C. Topp: *Low-Reynolds Number Effects in Ventilated Rooms: A Numerical Study*. 1395-7953 R0046.

PAPER NO. 122: F. Haghighat, H. Brohus, C. Frier, P. Heiselberg: *Stochastic Prediction of Ventilation System Performance*. ISSN 1395-7953 R0047.

PAPER NO. 123: H. Brohus, F. Haghighat C. Frier, P. Heiselberg: *Quantification of Uncertainty in Thermal Building Simulation. Part 1: Stochastic Building Model*. ISSN 1395-7953 R0048.

PAPER NO. 124: H. Brohus, F. Haghighat C. Frier, P. Heiselberg: *Quantification of Uncertainty in Thermal Building Simulation. Part 2: Stochastic Loads*. ISSN 1395-7953 R0049.

Complete list of papers: http://iee.civil.auc.dk/i6/publ/iee.html